Dynamics of intramolecular vibrational-energy redistribution (IVR). I. Coherence effects

Peter M. Felker[a] and Ahmed H. Zewail[b]
Arthur Amos Noyes Laboratory of Chemical Physics,[c] California Institute of Technology, Pasadena, California 91125

(Received 9 November 1984; accepted 17 December 1984)

In this series of papers, theoretical and experimental results concerning the dynamical manifestations of intramolecular vibrational-energy redistribution (IVR) in temporally resolved fluorescence are presented. In this paper (I) we present a general treatment of IVR and coherence effects in *multilevel* vibrational systems. Specifically, the concern is with the derivation of the characteristics of the beat-modulated fluorescence decays which arise from vibrational coupling among N levels within a molecule. Relations connecting quantum beat frequencies, phases, and modulation depths to coupling parameters are presented. Likely sources of deviation of experimental results from theoretical predictions are considered. And, finally, the direct link between IVR and time-resolved fluorescence experiments is discussed with emphasis placed on the physical interpretation of vibrational quantum beats and the nature of IVR as a function of vibrational energy in a molecule.

I. INTRODUCTION

The fundamental process of intramolecular vibrational energy redistribution (IVR) in isolated molecules involves the transfer of energy from a prepared initial state to other isoenergetic states. This *collisionless* redistribution of energy is the result of intramolecular couplings (anharmonic and/or Coriolis interactions) between rovibrational states. Spectral manifestations of IVR have been discussed previously and will not be addressed extensively here.[1] That which is of concern in this work involves the temporal characteristics of dispersed fluorescence on the picosecond time scale.[2] Our interest in these characteristics derives from the fact that the temporal behavior of a given fluorescence band is a direct view of the evolution of vibrational energy in the excited state vibrational manifold; from time- and frequency-resolved fluorescence measurements one can obtain information relating to the time scale of IVR, the nature (restricted or dissipative) of the process, and the coupling matrix elements involved.[3-5]

Recently, we have presented experimental results[3-5] on anthracene which illustrate the use of the picosecond technique in revealing IVR dynamics. There are, however, several relevant points that have not been addressed in detail concerning the dynamics of IVR in general, and its manifestations in the fluorescence decays of large molecules in particular. Firstly, there has been no comprehensive consideration of the consequences of *multilevel* vibrational coupling on IVR. Such consideration is especially essential to the understanding of restricted IVR (i.e., IVR among a few vibrational levels), as manifested in fluorescence decays as phase-shifted quantum beats.[3,4] Secondly, one would like to understand more about the changes in the nature of IVR as a function of vibrational energy in such multilevel systems. The parameters governing transitions from absent to restricted to dissipative IVR, as well as the sharpness of these transitions, are of interest. Thirdly, one might legitimately ask how it is possible to observe vibrational coherence effects (phase-shifted quantum beats) even though any given coupled vibrational level has associated with it a rotational level structure. With the large number of rovibrational states involved in the coupling between just two vibrational levels, one might think it likely that the superposition of the many different resulting beat frequencies would give rise to fluorescence decays with coherence effects completely smeared out. This is clearly not always the case. Thus, it remains to consider why this is so and what manifestations of the rotational level structure *are* present in a beat-modulated decay. Finally, it would be desirable to assess the generality of the concepts of IVR, which have been derived from the experimental observations made first on anthracene, to other molecules.

The purpose of this and the accompanying papers is to provide theoretical and experimental findings in an attempt to address the above points. Paper I gives a treatment of IVR and the coherence effects in multilevel IVR. These effects are related to experimental observables in time-resolved fluorescence studies. Paper II is a full account of experimental results on anthracene. Of particular concern in the paper are the changes in the nature of IVR as the excess vibrational energy changes and the identification of energy regions for restricted and dissipative IVR. Paper III deals with the role of rotations in IVR and the manifestations of rotational level structure in vibrational quantum beat-modulated decays. Finally, in paper IV we present experimental results taken for *trans*-stilbene to assess the generality of the anthracene results and the theoretical picture used to describe them.

Elsewhere,[3,4] we have presented initial theoretical and experimental studies of IVR in what we have termed

[a] IBM Graduate Fellow.
[b] Camille and Henry Dreyfus Foundation Teacher–Scholar.
[c] Contribution No. 7116.

 0021-9606/85/072961-14$02.10

the restricted limit. In particular, the dynamics of vibrational coupling among two or three vibrational levels has been considered. For these cases the manifestations of IVR in the temporal behavior of spectrally resolved fluorescence is relatively easy to recognize and interpret. In view of the expectation that vibrational coupling in molecules may involve any number of levels (especially at high energies) and that many such physical situations are amenable to study by picosecond spectroscopy, it would be useful to have some theoretical guidelines of the dynamical manifestations which a general system of N coupled vibrational levels might exhibit. In this paper (I) we derive and present such guidelines, discuss some possible deviations from the predicted behavior, and discuss the physical significance of the results. The results presented herein will be used in accompanying publications to interpret experimental observations made in this laboratory on the molecules anthracene (papers II and III)[6,7] and *trans*-stilbene (paper IV)[8] in the restricted and dissipative limits of IVR.

II. THEORY

A. General framework

We consider the case of N coupled vibrational levels in the S_1 manifold (Fig. 1). (Here we ignore the presence of the rotational level structure, the effects of which are discussed in paper III.[7]) These zero-order states, which we take to be products of one-dimensional harmonic oscillator wave functions, are denoted as $|a\rangle$, $|b\rangle$, $|c\rangle$, ... (In denoting a generic zero-order state, $|\gamma\rangle$ shall be used.) The molecular Hamiltonian matrix H, when expressed in this zero-order basis, is not diagonal because of coupling terms involving anharmonicity, etc. Diagonalization of H yields the molecular eigenstates $|1\rangle$, $|2\rangle$, $|3\rangle$, ..., (with energies E_1, E_2, E_3, ..., respectively), which are linear combinations of the zero-order states:

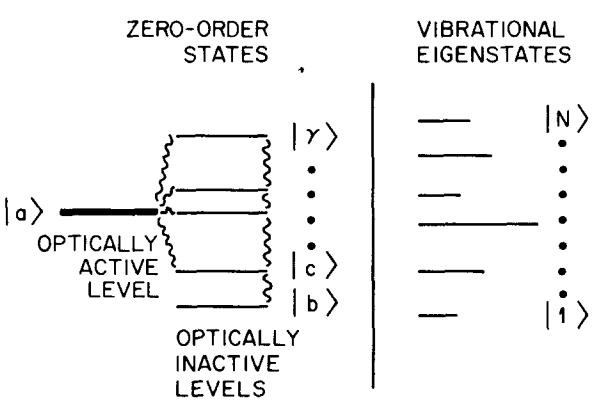

FIG. 1. Level diagram illustrating the general situation to be treated herein. The zero-order harmonic vibrational states on the left are coupled by anharmonic interactions. Only one of these states, the optically active $|a\rangle$ level, can be reached from the ground state via the excitation process. All of the other levels are optically inactive (dark). On the right are pictured the vibrational eigenstates that result from the interactions among the zero-order states. The different lengths of the lines representing these levels are meant to indicate that each eigenstate has a different contributuon from $|a\rangle$, and hence has a different absorption strength from the ground state.

$$|I\rangle = \sum_{\gamma=a,b,\cdots} \alpha_{I\gamma}|\gamma\rangle, \quad I = 1, \ldots, N, \tag{2.1}$$

where the $\alpha_{I\gamma}$ form a real,[9] orthonormal $N \times N$ matrix of the form:

$$C = \begin{pmatrix} \alpha_{1a} & \alpha_{2a} & \cdots & \alpha_{Na} \\ \alpha_{1b} & \alpha_{2b} & \cdots & \alpha_{Nb} \\ \cdot & \cdot & \cdot & \cdot \\ \cdot & \cdot & \cdot & \cdot \\ \cdot & \cdot & \cdot & \cdot \end{pmatrix}. \tag{2.2}$$

Now consider that a molecule in vibrational state $|g\rangle$ of the S_0 manifold is excited by a linearly polarized δ-function laser pulse (polarization vector $\hat{\epsilon}$) at the proper wavelength to create a coherent superposition of the molecular eigenstates $|I\rangle$, $I = 1, \ldots, N$. Such a coherent superposition of states will fluoresce to the levels $\{|f\rangle\}$ in the S_0 manifold. The fluorescence intensity vs time to one of these S_0 levels $|f_\gamma\rangle$ (assuming no analysis of fluorescence polarization) is given by[10]

$$I_\gamma(t) = K \sum_{I,J=1}^{N} \sum_{m=1}^{2} P_x(g, I)P_x(J, g) \times P_d^m(f_\gamma, J)P_d^m(I, f_\gamma)e^{-(i\omega_{IJ}+\Gamma)t}, \tag{2.3}$$

where K is a constant, $P_x(g, I) \equiv \langle g|\hat{\epsilon}\cdot\mu|I\rangle$ is the excitation transition matrix element connecting $|g\rangle$ and $|I\rangle$, $P_d^m(f_\gamma, I) \equiv \langle f_\gamma|\hat{\epsilon}_m\cdot\mu|I\rangle$ is a fluorescence transition matrix element connecting $|I\rangle$ and $|f_\gamma\rangle$, $\hat{\epsilon}_1$ and $\hat{\epsilon}_2$ are the two perpendicular fluorescence detection polarizations, $\omega_{IJ} \equiv (E_J - E_I)/\hbar$, and Γ is the decay rate of the excited eigenstates (taken for simplicity to be equal for all I[11]). *We call such a fluorescence band a γ-type band.*

In general, because of Franck–Condon factors and symmetry restrictions, only a limited number of the entire manifold of S_1 vibrational levels will have absorption strength from $|g\rangle$, as evidenced by the sharp and uncongested absorption and fluorescence excitation spectra of large jet-cooled molecules.[12] Thus, it is reasonable to take only one of the coupled zero-order levels as having any appreciable absorption strength from $|g\rangle$. *We take this level to be* $|a\rangle$. This leads to the following expression for $P_x(g, I)$:

$$P_x(g, I) = \alpha_{Ia}P_x(g, a) \quad \text{for} \quad I = 1, \ldots, N. \tag{2.4}$$

Similarly, one expects the Franck–Condon overlap for emission to the S_0 level $|f_\gamma\rangle$ to be dominated by one zero-order level $|\gamma\rangle$. In other words,

$$P_d^m(f_\gamma, I) = \alpha_{I\gamma}P_d^m(f_\gamma, \gamma) \quad \text{for} \quad I = 1, \ldots, N. \tag{2.5}$$

Substituting these expressions into Eq. (2.3) yields the following for the intensity vs time of a γ-type band:

$$I_\gamma(t) = K \sum_{I,J=1}^{N} \sum_{m=1}^{2} \alpha_{Ia}\alpha_{Ja}\alpha_{I\gamma}\alpha_{J\gamma} \times \{P_x(g, a)P_d^m(f_\gamma, \gamma)\}^2 e^{-(i\omega_{IJ}+\Gamma)t}, \tag{2.6a}$$

$$I_\gamma(t) = K'\left[\sum_{I=1}^{N} \alpha_{Ia}^2\alpha_{I\gamma}^2 + 2\sum_{I>J}^{N} \alpha_{Ia}\alpha_{Ja}\alpha_{I\gamma}\alpha_{J\gamma}\cos\omega_{IJ}t\right]e^{-\Gamma t}, \tag{2.6b}$$

where K' is a constant. [Note that if the fluorescence *were* analyzed for polarization—i.e., the sum over m were restricted in Eq. (2.6a)—exactly the same time dependence as Eq. (2.6b) would obtain for $I_\gamma(t)$. Only K' would change.[13]]

Now $|\gamma\rangle$ represents a generic zero-order state. Thus, one expects N different types of fluorescence bands in the fluorescence spectrum, each distinguished by the zero-order level which contributes to the emission transition moment. The time-integrated intensity of a given band type will scale with the quantity $\sum_{I=1}^{N}\alpha_{Ia}^2\alpha_{I\gamma}^2$. Moreover, from Eq. (2.6b) each of these bands will be modulated by the same $N(N-1)/2$ cosine modulation terms (quantum beats), the frequencies of which are determined by the energy differences between eigenstates, and the phases of which are determined by the particular band type via the coupling coefficients α. [One may further note that $\omega_{IJ}+\omega_{JK}=\omega_{IK}$. In general, $N(N-1)(N-2)/6$ such triplets of Fourier components are present for an N-level system when $N \geq 3$.] In what follows, we shall be interested in making generalizations concerning the amplitudes and the phases (i.e., signs) of quantities of the form

$$M_\gamma(\omega_{IJ}) \equiv \frac{2\alpha_{Ia}\alpha_{Ja}\alpha_{I\gamma}\alpha_{J\gamma}}{\sum_{I=1}^{N}\alpha_{Ia}^2\alpha_{I\gamma}^2}, \tag{2.7}$$

which from Eq. (2.6b) represents the modulation depth (normalized Fourier amplitude), for a γ-type band, of the Fourier component at frequency ω_{IJ}. Results for some specific values of N are presented in the Appendix.

B. Quantum beat modulation depths

There are several generalizations that can be made about the amplitudes of the modulation depths for a given band type. In making them it is necessary to distinguish between two types of fluorescence bands. The first type is the a-type band, which, using the conventions and nomenclature outlined above, represents a fluorescence band that derives its absorption and emission strength from the same zero-order state ($|a\rangle$). The second type of band is the non-a-type band, which by definition derives its absorption and emission strength from two different zero-order states ($|a\rangle$ and $|\gamma\rangle$, respectively).

For an a-type band, Eq. (2.7) reduces to

$$M_a(\omega_{IJ}) = \frac{2\alpha_{Ia}^2\alpha_{Ja}^2}{\sum_{I=1}^{N}\alpha_{Ia}^4}. \tag{2.8}$$

Since the α's are real, then $0 \leq 2\alpha_{Ia}^2\alpha_{Ja}^2 \leq \alpha_{Ia}^4+\alpha_{Ja}^4$. This places a restriction on the magnitude of each Fourier component contributing to an a-type band:

$$0 \leq M_a(\omega_{IJ}) \leq 1 \quad \text{for all} \quad \omega_{IJ}. \tag{2.9}$$

In addition to restrictions on individual components, it is also possible to place bounds on the sum of the modulation depths of an a-type band:

$$\sum_{I>J=1}^{N} M_a(\omega_{IJ}) = \frac{2\sum_{I>J=1}^{N}\alpha_{Ia}^2\alpha_{Ja}^2}{\sum_{I=1}^{N}\alpha_{Ia}^4}. \tag{2.10}$$

Such bounds derive from

$$\left(\sum_{I=1}^{N}\alpha_{Ia}^2\right)^2 = \sum_{I=1}^{N}\alpha_{Ia}^4 + 2\sum_{I>J=1}^{N}\alpha_{Ia}^2\alpha_{Ja}^2 = 1, \tag{2.11}$$

which yields

$$\sum_{I>J=1}^{N} M_a(\omega_{IJ}) = \frac{1}{\sum_{I=1}^{N}\alpha_{Ia}^4} - 1. \tag{2.12}$$

And, since $\sum_{I=1}^{N}\alpha_{Ia}^4$ is fixed by normalization such that $1/N \leq \sum_{I=1}^{N}\alpha_{Ia}^4 \leq 1$, then

$$0 \leq \sum_{I>J=1}^{N} M_a(\omega_{IJ}) \leq N-1. \tag{2.13}$$

For non-a-type bands one must treat the general form for $M_\gamma(\omega_{IJ})$ given by Eq. (2.7). Similar to a-type bands, one can place bounds on the magnitudes of individual modulation depths by noting that $|2\alpha_{Ia}\alpha_{Ja}\alpha_{I\gamma}\alpha_{J\gamma}| \leq \alpha_{Ia}^2\alpha_{I\gamma}^2+\alpha_{Ja}^2\alpha_{J\gamma}^2$ (this follows from $[\alpha_{Ia}\alpha_{I\gamma} \pm \alpha_{Ja}\alpha_{J\gamma}]^2 \geq 0$). Therefore, from Eq. (2.7),

$$0 \leq |M_\gamma(\omega_{IJ})| \leq 1 \quad \text{for all} \quad \omega_{IJ}, \quad \gamma \neq a. \tag{2.14}$$

Also, since

$$\sum_{I>J=1}^{N} M_\gamma(\omega_{IJ}) = \frac{2\sum_{I>J=1}^{N}\alpha_{Ia}\alpha_{Ja}\alpha_{I\gamma}\alpha_{J\gamma}}{\sum_{I=1}^{N}\alpha_{Ia}^2\alpha_{I\gamma}^2} \tag{2.15}$$

and

$$\left(\sum_{I=1}^{N}\alpha_{Ia}\alpha_{I\gamma}\right)^2 = \sum_{I=1}^{N}\alpha_{Ia}^2\alpha_{I\gamma}^2 + 2\sum_{I>J=1}^{N}\alpha_{Ia}\alpha_{Ja}\alpha_{I\gamma}\alpha_{J\gamma} = 0, \tag{2.16}$$

then

$$\sum_{I>J=1}^{N} M_\gamma(\omega_{IJ}) = -1, \quad \text{if} \quad \gamma \neq a. \tag{2.17}$$

That is, the sum of the modulation depths for any non-a-type band must equal -1.

C. Quantum beat phase distributions

Having considered some general restrictions on the magnitudes of the modulation depths of the Fourier components modulating the decay of a given band type, it is now useful to consider the phases of these components, or, equivalently, to consider the signs of the modulation coefficients. In particular, we are interested in generalizations that can be made concerning the possible distributions of quantum beat phases that can occur in a given decay. To address this task succinctly it is convenient to

start with several definitions. Firstly, we define $s_{I\gamma}$ to represent the sign of a given element of the orthonormal C matrix:

$$s_{I\gamma} \equiv \text{sign}(\alpha_{I\gamma}) = \pm 1. \tag{2.18}$$

Secondly, we define σ_γ to be an array of such quantities representing the signs of the γth row of C:

$$\sigma_\gamma \equiv (s_{1\gamma}, s_{2\gamma}, \ldots, s_{N\gamma}) = \text{sign}(\alpha_{1\gamma}, \alpha_{2\gamma}, \ldots, \alpha_{N\gamma}). \tag{2.19}$$

In similar fashion we define σ^I to be a column array of signs of the Ith column of C. Fourthly, we define $s_\gamma(\omega_{IJ})$ to be the phase of the Fourier component at frequency ω_{IJ} which modulates a γ-type band:

$$s_\gamma(\omega_{IJ}) \equiv \text{sign}[M_\gamma(\omega_{IJ})] = \pm 1. \tag{2.20}$$

Finally, we define Δ_γ to be the $1 \times [N(N-1)/2]$ dimensional array of quantum beat phases characterizing a γ-type band:

$$\Delta_\gamma \equiv [s_\gamma(\omega_{12}), s_\gamma(\omega_{13}), \ldots, s_\gamma(\omega_{1N}), s_\gamma(\omega_{23}), \ldots, s_\gamma(\omega_{N-1,N})]. \tag{2.21}$$

Next it is useful to make three observations concerning the arrays σ_γ and σ^I. The first observation is that one is free to choose all the values for one and only one of the arrays σ_γ. This freedom derives from the freedom to choose the phases of the eigenvectors composing the columns of C. It is convenient to use this to choose

$$\sigma_a = (+1, +1, +1, \ldots, +1). \tag{2.22}$$

Secondly and thirdly, we note that

$$\sigma_\gamma \neq \pm\sigma_{\gamma'} \quad \text{if} \quad \gamma \neq \gamma', \tag{2.23}$$

and that

$$\sigma^I \neq \pm\sigma^J \quad \text{if} \quad I \neq J. \tag{2.24}$$

These conditions follow from the orthogonality of the rows and columns of C, respectively.

We are now ready to consider the possible values of Δ_γ for an N-level system. Clearly,

$$\Delta_a = (+1, +1, +1, \ldots, +1), \tag{2.25}$$

for any system, since by Eq. (2.8),

$$s_a(\omega_{IJ}) = \text{sign}(\alpha_{Ia}^2\alpha_{Ja}^2) = +1 \quad \text{for all} \quad I, J. \tag{2.26}$$

In other words, a-type bands are only modulated by positive cosine terms [cf. Eq. (2.9)].

For non-a-type bands

$$s_\gamma(\omega_{IJ}) = \text{sign}(\alpha_{Ia}\alpha_{Ja}\alpha_{I\gamma}\alpha_{J\gamma}) = \text{sign}(\alpha_{I\gamma}\alpha_{J\gamma}) = s_{I\gamma}s_{J\gamma} \tag{2.27}$$

by our choice of eigenvector phases. Thus, the distribution Δ_γ is entirely determined by σ_γ for this choice of phases. One can now derive several conditions on the non-a-type phase distributions. Firstly, it is evident that all the values occurring in the quantum beat phase distribution array Δ_γ are not independent. If the values $s_\gamma(\omega_{1J})$, $J = 2, 3, \ldots, N$ are known, then since

$$s_\gamma(\omega_{1I})s_\gamma(\omega_{1J}) = (s_{1\gamma})^2 s_{I\gamma}s_{J\gamma} = s_\gamma(\omega_{IJ}), \tag{2.28}$$

it is clear that all other values in the array can be found, too. Thus, there are $N-1$ independent phases for a given band of an N-level system, and one can specify a phase distribution just by specifying the $1 \times (N-1)$ dimensional array:

$$\delta_\gamma \equiv [s_\gamma(\omega_{12}), s_\gamma(\omega_{13}), \ldots, s_\gamma(\omega_{1N})]. \tag{2.29}$$

Instead of working with the larger arrays Δ_γ, we shall equivalently consider the δ_γ arrays henceforth.

Secondly, it is evident from Eq. (2.27) that if σ_γ is nontrivially different from $\sigma_{\gamma'}$ then δ_γ is different from $\delta_{\gamma'}$, and vice versa. That is,

$$\sigma_\gamma \neq \pm\sigma_{\gamma'} \leftrightarrow \delta_\gamma \neq \delta_{\gamma'}. \tag{2.30}$$

Thirdly, this one to one correspondence between nontrivially different σ_γ and the resulting quantum beat phase distributions δ_γ, can be used along with Eq. (2.23) to show that for a given N-level system

$$\delta_\gamma \neq \delta_{\gamma'} \quad \text{if} \quad \gamma \neq \gamma'. \tag{2.31}$$

That is, each type of the N possible types of fluorescence bands that arise from an N-level system will have a unique quantum beat phase distribution.

Fourthly, one can use the correspondence between σ_γ and δ_γ to calculate the total possible number of different phase distributions for an N-level system. This can be done by calculating the number of nontrivially different σ_γ, which is

$$\frac{1}{2}\left[1 + N + \frac{N(N-1)}{2} + \frac{N(N-1)(N-2)}{6} + \cdots\right] = \frac{1}{2}(1+1)^N = 2^{N-1}. \tag{2.32}$$

Thus, there are 2^{N-1} possible values of δ_γ for N coupled levels. (We enumerate these possibilities for $N \leq 5$ below.) Note that all these possibilities are not realized for a given N-level system ($N \geq 3$), since only N bands occur in any given spectrum. Note also that we have not considered the restriction of Eq. (2.24) on the σ^I. It will be shown below that, although this does not restrict the possible values of δ_γ, it can restrict the possible combinations of δ_γ that can occur together in any given spectrum.

Fifthly, if one notes that the total number of distinct ways of distributing two values over $N-1$ variables is simply 2^{N-1}, then it is clear that the 2^{N-1} allowed δ_γ for an N level system represent *all the conceivable ways in which* $+1$ *and* -1 *can be distributed in these* $1 \times (N-1)$ *dimensional arrays.* As a consequence of this, it is very easy to write down all the possible δ_γ for a given system.

Finally, one can derive a general restriction on the distribution of quantum beat phases over the triplet of beat frequencies ω_{IJ}, ω_{JK}, $\omega_{IK}(=\omega_{IJ}+\omega_{JK})$. We define δ_γ^{IJK} to be such a distribution:

$$\delta_\gamma^{IJK} \equiv [s_\gamma(\omega_{IJ}), s_\gamma(\omega_{JK}), s_\gamma(\omega_{IK})], \quad (2.33)$$

and recall the expression for the $s_\gamma(\omega)$ (2.27). Now either $s_{I\gamma} = s_{J\gamma} = s_{K\gamma}$, or one of these three signs is different from the other two. The first possibility gives $\delta_\gamma^{IJK} = (+1, +1, +1)$, while the second can result in one of the three distributions $(+1, -1, -1)$, $(-1, +1, -1)$, or $(-1, -1, +1)$. Thus, out of the eight conceivable distributions, only the one with all positive phases and the three with two negative-one positive phase are actually possible.

D. Fluorescence spectra of band types

The fluorescence spectrum of a single *uncoupled* S_1 vibrational level of a large molecule exhibits, in general, a number of significantly intense bands. In other words, a given S_1 zero-order vibrational level has emission strength to more than just one S_0 level. In the fluorescence spectrum arising from an N-level system, therefore, one expects that there will be several bands present for each of the N band types. The spectral distribution of the fluorescence bands of a particular type can be predicted in large part for a given molecule just by knowing some features of the molecule's spectroscopy. The aim of this section is to present some predictions that can be made in this regard.

Let us start with several preliminary generalities. Firstly, for a given molecule, it is often true that one fluorescence spectral pattern is dominant and occurs in essentially all fluorescence spectra. This pattern is the 0^0-level fluorescence spectrum. Its ubiquity derives from the fact that for many S_1 single vibronic levels (SVL's) the strongest band in the fluorescence spectrum is that which corresponds to no change in vibrational quantum numbers in the transition from S_1 to S_0 (i.e., $\{\Delta v\} = 0$). (Note that such bands occur at about the same spectral position as the 0_0^0 band, but not at exactly the same place due to differences in S_1 and S_0 vibrational frequencies.) But this band serves as an origin for a 0^0-like spectrum, as is evident from consideration of the relevant Franck–Condon overlap integrals. Therefore, almost all S_1 zero-order vibrational levels give rise to fluorescence spectra which can be characterized, at least in part, as being 0^0-like fluorescence spectra with origins in the spectral region of the 0_0^0 transition.[12,14(b)]

The next point is that one can divide the vibrational normal modes of a molecule into two classes[14(b)]: (1) *optically active modes,* the vibrational quantum numbers of which can change in optical transitions between S_1 and S_0, and (2) *optically inactive modes,* the vibrational quantum numbers of which do not change in such transitions. This, in turn, leads to the classification of S_1 SVL's in terms of (1) *optically active levels,* the vibrational quantum numbers of which are only nonzero for optically active modes, and (2) *optically inactive levels,* which have some nonzero vibrational quantum numbers corresponding to optically inactive modes. Clearly, the fluorescence spectrum of an optically active level differs qualitatively from that of an inactive level. An active level can emit to the zero-point vibrational energy level of S_0 (i.e., 0_0), whereas an inactive level cannot. Moreover, progressions of optically active modes can be built off this particular band in an active level's spectrum, whereas in an inactive level's spectrum this does not occur.

A final preliminary point to be made is that the study of large molecule quantum beats virtually requires that the sample to be studied be a jet-cooled gas. Prior to excitation, such samples consist almost exclusively of molecules in the 0_0 vibrational level. Therefore, by our definition of the $|a\rangle$ state as one which has absorption strength, it is apparent that all the nonzero quantum numbers characterizing $|a\rangle$ belong to optically active modes; that is, $|a\rangle$ is an optically active level. On the other hand, the states which couple to $|a\rangle$ and which do not have significant absorption strength from 0_0 must involve some quanta in inactive modes. Therefore, these states correspond to optically inactive levels.

Now, we are in a position to consider the spectral distributions of various band types. Since $|a\rangle$ is an active level and all other $|\gamma\rangle$ are inactive levels, one expects that the bluest band in the spectrum of an N-level system, the resonance fluorescence band (for cold molecules), will be a type and that all progressions of optically active modes built on this band will also be a type.

On the other hand, the spectra of non-a-type fluorescence bands, since they arise from optically inactive levels, will be different. It is convenient to divide non-a-type bands into two classes based on whether the zero-order state giving them their emission strength ($|\gamma\rangle$) has any nonzero optically active quantum numbers or not. If all the optically active quantum numbers are zero for $|\gamma\rangle$, then the spectrum arising from $|\gamma\rangle$ is simply a 0^0-like spectrum with an origin in the region of the 0_0^0 band position. This origin is the band corresponding to $\{\Delta v\} = 0$. (Note that the shift of this band from the a-type resonance fluorescence band will not correspond to any interval associated with optically active modes.) If some of the optically active quantum numbers are nonzero for $|\gamma\rangle$, then the situation is more complex. In this case, one still expects the γ-type spectrum to be composed, in part, of a 0^0-like spectrum with an origin ($\{\Delta v\} = 0$) in the 0_0^0 region. However, the possibility also exists that there will be significantly intense γ-type bands to the blue of this which correspond to transitions where $\{\Delta v\} < 0$. These bands will be separated from the γ-type $\{\Delta v\} = 0$ band by intervals associated with optically active modes, and, of course, they will not be as far to the blue as the resonance fluorescence a-type band.

The different characteristic spectral distributions of a-type vs non-a-type bands leads to a rough division of an N-level fluorescence spectrum into two regions[5,12,14] (see Fig. 2). The so-called vibrationally unrelaxed region is that part of the spectrum which occurs to the blue of the 0_0^0 band position and which includes the resonance fluorescence. This region consists predominantly of a-type bands. To the red of this is the vibrationally relaxed region, which is composed primarily of the superposition of all the 0^0-like spectra arising from the states coupled to $|a\rangle$.

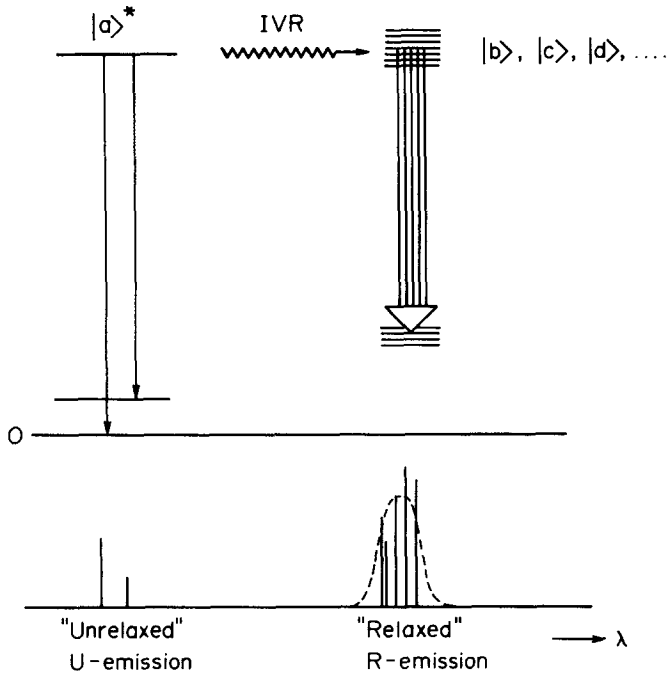

FIG. 2. Level diagram and fluorescence spectrum representing the dispersed fluorescence characteristics to be expected from a set of coupled vibrational levels in S_1. Excitation prepares the zero-order $|a\rangle$ state (indicated by the asterisk) which then undergoes IVR. Emission gaining its strength from $|a\rangle$ is termed vibrationally unrelaxed and tends to occur in the blue region of the spectrum. Emission gaining its strength from $|b\rangle$, $|c\rangle$, ..., is termed vibrationally relaxed and occurs near and to the red of the 0_0^0 transition energy of the molecule.

III. QUANTUM BEAT PARAMETERS AND THE DETERMINATION OF H_0

We have noted before,[3] and show in the Appendix to this paper, that observed quantum beat parameters for $N = 2$ can be used to calculate parameters associated with the Hamiltonian matrix expressed in the zero-order basis (i.e., H_0). This can also be done for $N \geq 3$. Unlike $N = 2$, however, expressions for the parameters of H_0 cannot be conveniently presented for $N \geq 3$. Nevertheless, a general method can be outlined by which a calculation of H_0 can be performed[15] given measured beat frequencies and modulation depths. We present here such an outline for $N = 3$. Extension of the method to larger values of N is straightforward. The calculation of H_0 using real data taken on anthracene will be presented in the following paper (II).

The basis of the method of calculation is the relation

$$CEC^t = H_0, \tag{3.1}$$

which relates the eigenvalue matrix E, the eigenvector matrix C, and the transpose of the eigenvector matrix C^t to H_0. Now the eigenvalue matrix is partially determined by the beat frequencies. If one labels the frequencies such that $|\omega_{12}| + |\omega_{23}| = |\omega_{13}|$, then the following possibilities exist for E:

$$E = E_0 I \pm \begin{pmatrix} 0 & 0 & 0 \\ 0 & |\omega_{12}| & 0 \\ 0 & 0 & |\omega_{13}| \end{pmatrix}, \tag{3.2}$$

where E_0 is an unknown constant and I is the unit matrix.

The eigenvector matrix C can be determined from relative values of the $M_\gamma(\omega_{IJ})$'s and from the orthonormality of its rows and columns. Firstly, it is convenient to calculate the α_{Ia} via the relations

$$\alpha_{2a}^2 = \frac{M_a(\omega_{23})}{M_a(\omega_{13})}\,\alpha_{1a}^2, \tag{3.3a}$$

$$\alpha_{3a}^2 = \frac{M_a(\omega_{23})}{M_a(\omega_{12})}\,\alpha_{1a}^2, \tag{3.3b}$$

and the normalization relation $\sum_{I=1}^3 \alpha_{Ia}^2 = 1$. The signs of the α_{Ia} can be arbitrarily chosen to be positive. Next, the values α_{Ib} can be calculated by the relations

$$\alpha_{2b} = \frac{M_b(\omega_{23})\alpha_{1a}}{M_b(\omega_{13})\alpha_{2a}}\,\alpha_{1b}, \tag{3.4a}$$

$$\alpha_{3b} = \frac{M_b(\omega_{23})\alpha_{1a}}{M_b(\omega_{12})\alpha_{3a}}\,\alpha_{1b}, \tag{3.4b}$$

and the normalization condition $\sum_{I=1}^3 \alpha_{Ib}^2 = 1$. Note that the *relative* signs of the α_{Ib} are fixed by the beat phases of the b-type band [e.g., if $\delta_b = (-1, +1)$, then $\sigma_b = \pm(+1, -1, +1)$]. Thus, the second row of C is determined up to an overall sign. Finally, the values α_{Ic} can be calculated up to an overall sign by using several relations, including the normality of the columns of C and the orthogonality of its rows.

One may note that the values of the elements of C are overspecified if one has experimental knowledge of all the quantum beat modulation depths for all three types of bands. The extra parameters can be used as self-consistency checks on the calculated C. For instance, absolute modulation depths were not used at all in the calculation outlined above, nor were the modulation depths and phases of the c-type band. These experimental values should, however, be reproduced if one calculates them starting with the derived C. Similarly, a number of orthogonality and normality relations (e.g., $\sum_{I=1}^3 \alpha_{Ia}\alpha_{Ib} = 0$) need not figure in the calculation of C. These relations should, nevertheless, obtain if the calculated matrix accurately represents the physical situation.

Now, it being clear that one can determine C and E up to various additive and multiplicative constants, what can be determined for H_0? Firstly, by Eqs. (3.1), (3.2), and the orthonormality of C,

$$H_0 = E_0 I \pm C \begin{pmatrix} 0 & 0 & 0 \\ 0 & |\omega_{12}| & 0 \\ 0 & 0 & |\omega_{13}| \end{pmatrix} C^t. \tag{3.5}$$

Next, the effect of the ambiguities in the overall signs of the rows of C must be considered. Since $h_{\gamma\gamma'}$, a general matrix element of the second term on the right-hand side of Eq. (3.5) is

$$h_{\gamma\gamma'} = h_{\gamma'\gamma} = \alpha_{2\gamma}\alpha_{2\gamma'}|\omega_{12}| + \alpha_{3\gamma}\alpha_{3\gamma'}|\omega_{13}|, \tag{3.6}$$

it is clear that changing the overall signs of the γth row of C will leave the diagonal element $h_{\gamma\gamma}$ unchanged, but

will change the signs of those off-diagonal elements involving γ. From this fact and Eq. (3.5), it is evident that by using quantum beat parameters, one can obtain

$$H_0 = E_0 I \pm \begin{pmatrix} E_a & V_{ab} & V_{ac} \\ V_{ab} & E_b & V_{bc} \\ V_{ac} & V_{bc} & E_c \end{pmatrix}, \tag{3.7}$$

where E_0 and the signs of the $V_{\gamma\gamma'}$ are unknown, but everything else is known.

IV. EXPERIMENTAL RESULTS VS THEORETICAL PREDICTIONS

To handle real data it is useful to have some idea of the way in which the theoretical results, which have been derived using a set of ideal assumptions, can be modified by less than ideal conditions. In this section we discuss effects which the experimental excitation bandwidth, the temporal response of detection, the spectral resolution of detection, the excitation of more than one optically active level, and the presence of sequence congestion can have on experimental observations. Since in many cases these deviations can lead to errors in interpretation, especially in the interpretation of the number of levels involved in the coupling, we suggest ways to avoid such errors. No attempt will be made to be exhaustive in the enumeration of all the causes of possible deviations. Instead, several cases will be presented in the expectation that they represent a significant fraction of those cases likely to be encountered in practice, and in the hope that they will illustrate methods of analysis by which other cases may be treated. Reference to a number of the cases presented here is made in the accompanying papers in discussing real experimental results.

A. Case 1: Narrow excitation bandwidth and state preparation

In this case we assume that the bandwidth of the experimental source is not large enough to coherently excite all the N eigenstates which arise from the coupling of the N zero-order levels (Fig. 3). This situation is likely to occur in real molecules, since anharmonic coupling

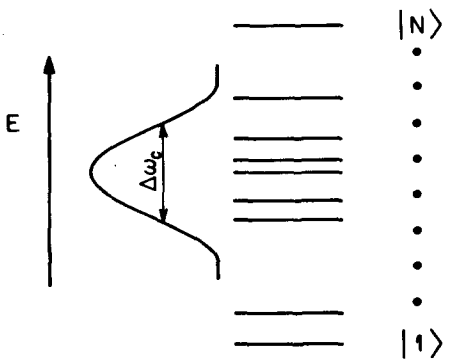

FIG. 3. Schematic diagram of the situation treated as case 1 (Sec. IV A), wherein it is assumed that the bandwidth ($\Delta\omega_c$) of the excitation source is not large enough to span all the eigenstates ($|1\rangle, \ldots, |N\rangle$) resulting from the coupling of a set of N zero-order states.

matrix elements may be expected to be as high as several wavenumbers and to therefore give rise to significantly coupled states with splittings on this order.

For simplicity, let us say that one state $|N\rangle$ lies outside the laser bandwidth. In such a case, N band types are still possible, but the temporal behavior of a γ-type band will be given by

$$I_\gamma(t) \sim \sum_{I,J=1}^{N-1} \alpha_{Ia}\alpha_{Ja}\alpha_{I\gamma}\alpha_{J\gamma} e^{-(i\omega_{IJ}+\Gamma)t} \tag{4.1}$$

instead of by Eq. (2.6). Thus, although the system involves N coupled zero-order levels, each band will be modulated by the number of beat frequencies expected for an $(N-1)$-level system. (In the general case wherein n eigenstates lie outside the laser bandwidth, the number of band types will still be N, but the number of beat frequencies will correspond to that expected for an $N-n$ level system.) Fortunately, another deviation from theoretical predictions can be used to give one an idea of the actual number of coupled zero-order levels. If one calculates the total modulation depth of a γ-type band (non-a-type) from Eq. (4.1), one obtains

$$\sum_{I>J=1}^{N-1} M_\gamma(\omega_{IJ}) = \frac{2\sum_{I>J=1}^{N-1} \alpha_{Ia}\alpha_{Ja}\alpha_{I\gamma}\alpha_{J\gamma}}{\sum_{I=1}^{N-1} \alpha_{Ia}^2\alpha_{I\gamma}^2}. \tag{4.2}$$

Given that $\sum_{I=1}^{N-1} \alpha_{Ia}\alpha_{I\gamma} \neq 0$, then clearly,

$$\left(\sum_{I=1}^{N-1} \alpha_{Ia}\alpha_{I\gamma}\right)^2 = \sum_{I=1}^{N-1} \alpha_{Ia}^2\alpha_{I\gamma}^2 + 2\sum_{I>J=1}^{N-1} \alpha_{Ia}\alpha_{Ja}\alpha_{I\gamma}\alpha_{J\gamma} > 0, \tag{4.3}$$

and, therefore,

$$\sum_{I>J=1}^{N-1} M_\gamma(\omega_{IJ}) = \frac{2\sum_{I>J=1}^{N-1} \alpha_{Ia}\alpha_{Ja}\alpha_{I\gamma}\alpha_{J\gamma}}{\sum_{I=1}^{N-1} \alpha_{Ia}^2\alpha_{I\gamma}^2} > -1. \tag{4.4}$$

(Note that the relation $\sum_{I>J=1}^{N_0} M_\gamma(\omega_{IJ}) > -1$, for $N_0 < N$, holds in general.) Equation (4.4) contrasts with the rule given by Eq. (2.17). Thus, the measured total modulation depth of a non-a-type band provides a measure by which one can decide if the number of levels indicated by the number of beat frequencies is, in fact the total number of coupled levels. (This, of course, assumes the ability to accurately measure modulation depths.) This same information would also be obtained if the beat phase distributions indicated that more than $N-1$ types of bands occurred in the spectrum.

In terms of the physics of IVR, case 1 corresponds to the incomplete preparation of the $|a\rangle$ state at $t = 0$. In other words, the initially prepared state is not purely $|a\rangle$ as it would be if the bandwidth of the laser spanned all the eigenstates arising from the coupled system of zero-order states (see Sec. V A), but it contains contributions

from the other zero-order states, as well. The deviations resulting from the case 1-type situation are therefore fundamental in nature and underscore the fact that the IVR process is intimately dependent on the preparation of the initial state.

B. Case 2: Finite temporal resolution

In this case we assume that the temporal resolution of the detection system is not sufficient to resolve some of the beat frequencies present in the decays. Obviously, under all circumstances the inability to resolve some beat components reduces the number of observed beat frequencies from the $N(N-1)/2$ expected for N coupled levels. In many cases this will not lead to an incorrect assignment of the number of coupled levels involved. For instance, if for a four-level system only five beat frequencies were resolvable, then despite the missing component, one would not be led to assign the behavior to a three-level system, since in that case there would be only three beat components. Similarly, if one observed three beat components at say 5, 7, and 8 GHz, it would be immediately apparent that the number of coupled levels involved would have to exceed three, since $5+7 \neq 8$ GHz. On the other hand, errors in interpretation *can* be made if the only beat frequencies that are unresolvable are all those involving one of the eigenstates. For example, say all ω_{IN}, for $I=1, \ldots, N-1$, are too large. In such a case each band will be apparently modulated as if it arose from an $(N-1)$-level system:

$$I_\gamma(t) \sim \left[\sum_{I=1}^{N} \alpha_{Ia}^2 \alpha_{I\gamma}^2 + 2 \sum_{I>J=1}^{N-1} \alpha_{Ia}\alpha_{Ja}\alpha_{I\gamma}\alpha_{J\gamma} \cos \omega_{IJ} t\right] e^{-\Gamma t}. \tag{4.5}$$

Nevertheless, here as with case 1, errors in interpretation can, in principle, be avoided by consideration of the total modulation depths of non-a-type bands

$$\sum_{I>J=1}^{N-1} M_\gamma(\omega_{IJ}) = \frac{2 \sum_{I>J=1}^{N-1} \alpha_{Ia}\alpha_{Ja}\alpha_{I\gamma}\alpha_{J\gamma}}{\sum_{I=1}^{N} \alpha_{Ia}^2 \alpha_{I\gamma}^2}. \tag{4.6}$$

Since Eq. (4.6) is the same as Eq. (4.2) except for one extra positive term in the denominator, then the sum of modulation depths in Eq. (4.6) is ≥ -1. Thus, this experimentally measurable quantity can again be used to ascertain whether the apparent number of coupled levels is, in fact, the actual number of coupled levels.

C. Case 3: Finite spectral resolution

Similar to effects due to finite temporal resolution, one might expect spectral detection resolution problems to be an especially prevalent source of experimental deviations from the theoretical predictions of Sec. II. Even single, nonvibrationally coupled S_1 vibrational levels of large molecules (for instance, the S_1 vibrationless level) have rich spectra with many bands. Since an N-level system is a superposition of such spectra, there is bound to be some spectral overlap of bands, even for N as small as three. This overlap can result in a number of apparent deviations from theoretical predictions. For example, if an a-type band overlaps with a non-a-type band, then the measured decay may appear to be non-a-type because of Fourier components with -1 phases, yet the total modulation depth of the decay will be found to be ≥ -1. Or, if two different non-a-type bands overlap, then it is possible that the measured decay may exhibit forbidden phase behavior, e.g., a quantum beat triplet may appear to have a phase distribution

$$\delta_\gamma^{IJK} = (+1, +1, -1).$$

Clearly, spectral overlap can also be an especially serious hindrance if one wishes to obtain accurate modulation depths for a calculation of H_0. This must be kept in mind in choosing the experimental results to be used in making such a calculation.

D. Case 4: More than one optically active level, uncoupled

As a fourth case, consider the situation wherein the eigenstates formed by the coupling of the M zero-order states $|a\rangle$, $|b\rangle$, $\cdots$ *and* the eigenstates formed by the coupling of the $N-M$ zero-order states $|a'\rangle$, $|b'\rangle$, $\cdots$ are all spanned by the finite bandwidth of the laser pulse. Assume that the unprimed zero-order states are only coupled to other unprimed states and give rise to the eigenstates $|I\rangle$, $I=1, \ldots, M$; while the primed states are only coupled to primed states and in so doing give rise to the eigenstates $|I\rangle$, $I=M+1, \ldots, N$; (see Fig. 4). In such a situation C is block diagonalized into two blocks such that all the elements $\alpha_{I\gamma}$ are zero if (1) γ is unprimed and $I=M+1, \ldots, N$ or (2) γ is primed and $I=1, \ldots, M$. Now, further assume that only one zero-order state in each set (say $|a\rangle$ and $|a'\rangle$) has any absorption strength from the populated S_0 level. Using Eq. (2.3) one can obtain the following for the temporal behavior of the

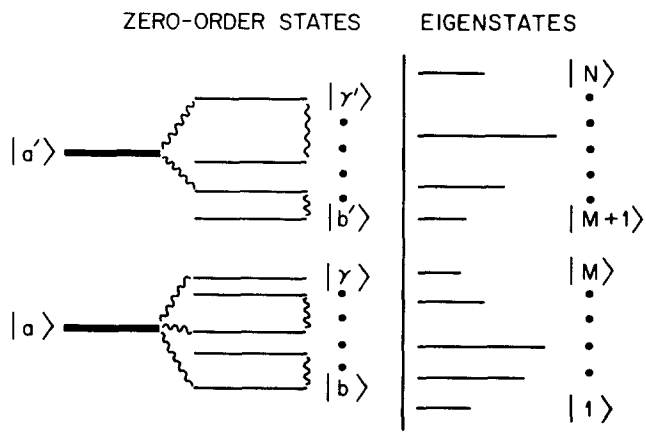

FIG. 4. Schematic diagram of the situation treated as case 4 (Sec. IV D), wherein it is assumed that the laser bandwidth is large enough to excite the eigenstates (right) corresponding to two independent (noninteracting) sets of coupled zero-order levels (left). Only two zero-order levels are assumed to have absorption strength from the ground state—the $|a\rangle$ and $|a'\rangle$ states.

fluorescence band associated with the transition to the S_0 level $|f_\gamma\rangle$:

$$I_\gamma(t) = I_\gamma^1 + I_\gamma^2 + I_\gamma^3, \tag{4.7a}$$

where

$$I_\gamma^1 \sim \sum_{I,J=1}^{M} \sum_{m=1}^{2} \alpha_{Ia}\alpha_{Ja} P_d^m(f_\gamma, J) P_d^m(f_\gamma, I) e^{-(i\omega_{IJ}+\Gamma)t}, \tag{4.7b}$$

$$I_\gamma^2 \sim \sum_{I,J=M+1}^{N} \sum_{m=1}^{2} \alpha_{Ia'}\alpha_{Ja'} P_d^m(f_\gamma, J) P_d^m(f_\gamma, I) e^{-(i\omega_{IJ}+\Gamma)t}, \tag{4.7c}$$

and

$$I_\gamma^3 \sim 2 \sum_{I=1}^{M} \sum_{J=M+1}^{N} \sum_{m=1}^{2} \alpha_{Ia}\alpha_{Ja'} P_d^m(f_\gamma, J) \times P_d^m(f_\gamma, I)\cos(\omega_{IJ}t) e^{-\Gamma t}. \tag{4.7d}$$

As before, we assume that the transition to $|f_\gamma\rangle$ gains its emission strength from only one of the zero-order levels. Unlike before, however, one sees from Eq. (4.7) that all N band types are not modulated by all the same beat frequencies. In fact, three different classes of band types can be distinguished based on the frequencies which modulate the bands. Firstly, if the band gains its emission strength from one of the unprimed zero-order states, then $S_\gamma^2 = S_\gamma^3 = 0$ and S_γ^1 reduces to what one would expect for a band of an M-level system. One expects as many as M types of bands exhibiting such behavior. Similarly, if the band gains its emission strength from one of the primed zero-order states, then $S_\gamma^1 = S_\gamma^3 = 0$ and S_γ^2 reduces to what one would expect for a band arising from an $(N - M)$-level system. As many as $N - M$ bands of this type may occur. Finally, there will be at least one band (i.e., the resonance fluorescence band) which gains its emission strength from $|a\rangle$ and $|a'\rangle$. $I_\gamma(t)$ for such a band will have contributions from S_γ^1, S_γ^2, and S_γ^3. Thus, all $N(N-1)/2$ beat frequencies of the N-level system may modulate the band. Moreover, all these Fourier components will have +1 phases since α_{Ia} and/or $\alpha_{Ia'}$ only enter as squared terms in S_γ^1, S_γ^2, and S_γ^3.

The situation corresponding to case 4 is not particularly unlikely to occur. For example, one can easily imagine two sets of states at the same energy having different symmetry transformation properties. While interset anharmonic coupling in such a case would be symmetry forbidden, absorption could still occur to states in both of the sets (e.g., in anthracene S_1 vibrational levels of both a_g and b_{1g} symmetry have been observed to be optically active[12]).

E. Case 5: More than one optically active level, coupled

Here, we consider a situation which gives rise to deviations from theory, not because of any experimental limitations, but because the physical situation does not correspond to the basic assumptions of the theory. In particular, we consider the case wherein there are no restrictions on the absorption transition matrix elements $P_x(g, I)$ or on the emission transition matrix elements $P_d^m(f_\gamma, I)$ in Eq. (2.3); that is, Eqs. (2.4) and (2.5) do not hold. Since this general case is difficult to treat for any but the simplest systems, we only present results for $N = 2$.

As in Sec. II A, it is useful here to express the transition matrix elements in terms of the zero-order states $|a\rangle$ and $|b\rangle$. We also neglect the effects of detection polarization. Thus,

$$P_x(g, I) = \alpha_{Ia}P_x(g, a) + \alpha_{Ib}P_x(g, b) \tag{4.8}$$

and

$$P_d(f, I) = \alpha_{Ia}P_d(f, a) + \alpha_{Ib}P_d(f, b). \tag{4.9}$$

For the sake of clarity we define $X_\gamma \equiv P_x(g, \gamma)$ and $D_\gamma \equiv P_d(f, \gamma)$. Using the facts[16] that $\alpha_{1a} = -\alpha_{2b} = \alpha$ and $\alpha_{2a} = \alpha_{1b} = \beta$ along with Eq. (2.3) to find the decay of the fluorescence band with final state $|f\rangle$, one obtains the following for the modulation depth of the beat component ω_{12}:

$$M(\omega_{12}) = \frac{2(\alpha X_a + \beta X_b)(\beta X_a - \alpha X_b)(\alpha D_a + \beta D_b)(\beta D_a - \alpha D_b)}{(\alpha X_a + \beta X_b)^2(\alpha D_a + \beta D_b)^2 + (\beta X_a - \alpha X_b)^2(\beta D_a - \alpha D_b)^2}. \tag{4.10}$$

It is apparent from Eq. (4.10) that the general case differs from that of Sec. II in that modulation depths do not solely depend on the coupling coefficients but are dependent on zero-order transition matrix elements, as well. Even in a two-level system, one might therefore expect many different fluorescence bands, each with different $M(\omega_{12})$ depending on the particular values of D_a and D_b for the band. In addition, the possibility exists, despite strong coupling between $|a\rangle$ and $|b\rangle$, that no modulations will appear in any decays if X_a and X_b, or D_a and D_b take on certain values.

It is instructive to consider two limiting cases of Eq. (4.10). In particular, one wonders what happens if either D_a or D_b is equal to zero, but both the X_γ have nonzero values. This corresponds to the case of two *coupled* optically active levels which have different fluorescence spectra. If one detects the band for which D_b equals zero, one has what is analogous to an a-type band, the modulation depth of which is

$$M_a(\omega_{12}) = \frac{2(\alpha X_a + \beta X_b)(\beta X_a - \alpha X_b)\alpha\beta}{(\alpha X_a + \beta X_b)^2\alpha^2 + (\beta X_a - \alpha X_b)^2\beta^2}. \tag{4.11}$$

With D_a equal to zero one obtains

$$M_b(\omega_{12}) = \frac{-2(\alpha X_a + \beta X_b)(\beta X_a - \alpha X_b)\alpha\beta}{(\alpha X_a + \beta X_b)^2\beta^2 + (\beta X_a - \alpha X_b)^2\alpha^2}. \quad (4.12)$$

Comparing Eqs. (4.11) and (4.12), one can see that the decays of the two types of bands have opposite quantum beat phases (+1 vs −1) just as in the two-level case of Eq. (2.3). Now, however, that decay which has the −1 phase cannot be predicted without specific knowledge of the coupling coefficients *and* the X_γ. The same holds true for the magnitudes of $M_a(\omega_{12})$ and $M_b(\omega_{12})$. In general, one expects the modulation depths to decrease with both weaker coupling and with $|X_a|$ more nearly equal to $|X_b|$. One also expects no decay for which the modulation depth equals −1 [in contrast to Eq. (2.17)].

It is implicit to the relevance of this paper that in many real situations the approximations of Eqs. (2.4) and (2.5) be good ones and that case 5 be an overcomplication. As we have argued, theoretical considerations and experimental results support this. Given cases for which Eqs. (2.4) and (2.5) are not valid, one sees from Eqs. (4.10)–(4.12) that even for $N = 2$ significant deviations from the results of Sec. II (and the Appendix) can occur.

F. Case 6: Thermal congestion

A primary assumption made in the treatment of Sec. II involves the presence of only one initially populated S_0 state ($|g\rangle$). However, even in jet-cooled samples there exists a distribution of initial states due to incomplete cooling of both rotational and vibrational degrees of freedom. This distribution of initial states can in turn give rise to a distribution of excited states upon laser excitation. The effects that a distribution of excited state rotational levels has on beat-modulated decays are dealt with in paper III.[7] The influence of the vibrational distribution, although not as pervasive as that of the rotational distribution, nevertheless can be substantial. For instance, consider a vibrational distribution characterized by some molecules in the S_0 level $|g_1\rangle$ and all others in the level $|g_2\rangle$. Excitation will project the two types of molecules up into entirely different regions of the excited state level structure given that $|g_1\rangle$ and $|g_2\rangle$ are well separated in energy relative to the bandwidth of the laser pulse. Spectrally, the effect this has is to introduce more congestion in the observed fluorescence spectrum than would otherwise be present if all molecules were initially in $|g_1\rangle$ or $|g_2\rangle$. Temporally, if excitation from $|g_1\rangle$ coherently prepares an N_1-level system and excitation from $|g_2\rangle$ prepares an N_2-level system, then there will be bands in the observed fluorescence spectrum reflecting coupling among N_1 levels, and different bands reflecting coupling among N_2 levels. The point is that two different and independent dynamical processes arising from two incoherently related excitations are manifested in the observed spectrum and fluorescence decays. Thus, in cases where observations indicate deviations from theoretical predictions regarding the number of beat components and the number of beat triplets, it is possible that the reason for this is vibrational thermal congestion. In the extreme situations where many S_0 vibrational states are initially populated, thermal congestion can completely mask any coherence effects that may be present. Of course, this at the heart of the rationale to use jet-cooled molecular samples in the study of large molecule vibrational dynamics. Experimental results pertaining to the effects of thermal congestion are presented in paper III.[7]

V. PHASE-SHIFTED QUANTUM BEATS AND IVR

A. Direct view of IVR

Being that phase-shifted quantum beats occur as one of the dynamical manifestations of S_1 vibrational coupling in molecules and that the specific characteristics of observed beats can be used to obtain specific vibrational coupling information about a molecule, then the study of phase-shifted vibrational beats amounts to the study of IVR. However, the connection between beats and IVR is even closer than this might lead one to believe. Far from being simple dynamical manifestations of vibrational coupling, beat-modulated fluorescence decays are direct pictures of the distribution in time of vibrational energy in a molecule. This point may be seen by considering the contribution $[\rho_\gamma(t)]$ of the zero-order state $|\gamma\rangle$ to the excited state $|\Psi(t)\rangle$ created by the laser pulse:

$$\rho_\gamma(t) = |\langle\gamma|\Psi(t)\rangle|^2. \quad (5.1)$$

Using the assumptions of δ function excitation and the exclusive absorption strength of $|a\rangle$ one obtains for the normalized excited state

$$|\Psi(t)\rangle = \sum_{I=1}^{N} \alpha_{Ia}|I\rangle e^{-(i\omega_I+\Gamma/2)t}$$

$$= \sum_{I=1}^{N} \sum_{\gamma=a,b,\cdots} \alpha_{Ia}\alpha_{I\gamma}|\gamma\rangle e^{-(i\omega_I+\Gamma/2)t}. \quad (5.2)$$

And using Eq. (5.2),

$$\rho_\gamma(t) = \left|\sum_{I=1}^{N} \alpha_{Ia}\alpha_{I\gamma}e^{-(i\omega_I+\Gamma/2)t}\right|^2$$

$$= \sum_{I,J=1}^{N} \alpha_{Ia}\alpha_{Ja}\alpha_{I\gamma}\alpha_{J\gamma}e^{-(i\omega_{IJ}+\Gamma)t}. \quad (5.3)$$

[Actually, the requirement of a δ-function excitation pulse is somewhat restrictive. A more realistic condition is that the inverse correlation time of the excitation source—the coherence width—be much greater than the maximum value of ω_{IJ}. This same condition, which ensures that all of the relevant eigenstates are excited and locked in phase at $t = 0$, also applies to Eq. (2.6). Comprehensive discussions on the question of initial state preparation can be found in Refs. 10 and 17.]

By comparison of Eq. (5.3) with Eq. (2.6), it is evident that

$$\rho_\gamma(t) \sim I_\gamma(t). \quad (5.4)$$

The temporal behavior of a γ-type band is exactly the same as the temporal behavior of the $|\gamma\rangle$ content of the excited state. In another manner of speaking, a γ-type

decay provides a direct picture of the oscillatory flow of energy into and out of the vibrational motion described by $|\gamma\rangle$. Thus, the two fundamental aspects of the IVR process can be addressed by time- and frequency-resolved fluorescence. The *extent* of IVR (the number of coupled vibrational levels) is given by the number of beat frequencies which modulate the decays of the bands in a spectrum, and the *time scale* for energy redistribution is given by the inverses of the beat frequencies.

There are other ways in which the correspondence between $I_\gamma(t)$ and $\rho_\gamma(t)$ can be useful in the study of IVR processes. For example, Eq. (5.4) allows one to carry all the theoretical results on the modulation phases and modulation depths of fluorescence decays (Sec. II and the Appendix) over to the behavior of $\rho_\gamma(t)$. Conversely, if one first considers the behavior of $\rho_\gamma(t)$, which has a ready interpretation in terms of IVR, then it is possible to come to a fuller appreciation of the physical significance of some of the results derived for $I_\gamma(t)$. One example of this point is Eq. (2.17), which holds that the total modulation depth of a non-a-type decay is -1. What does this mean physically? To answer this note from Eq. (5.3) that for $\gamma \neq a$,

$$\rho_\gamma(0) = \sum_{I,J=1}^{N} \alpha_{Ia}\alpha_{Ja}\alpha_{I\gamma}\alpha_{J\gamma} = \sum_{I=1}^{N}\left(\sum_{J=1}^{N}\alpha_{Ja}\alpha_{J\gamma}\right)\alpha_{Ia}\alpha_{I\gamma} = 0 \tag{5.5}$$

by orthogonality. That is, $|\gamma\rangle$ does not contribute to the initially prepared excited state. Now by Eq. (5.4) this implies that $I_\gamma(0) = 0$, which in turn, by Eqs. (2.6) and (2.7) implies that the total modulation depth of the γ-type band must be -1. Thus, the modulation depth sum rule (2.17) for non-a-type bands is a reflection of the vibrational content of the initially prepared excited state. Similarly, the fact that an a-type band is modulated exclusively by beats with positive phases is a reflection of the vibrational content of $|\Psi(t)\rangle$ at $t = 0$. By Eq. (5.3) and the normalization of the α_{Ia},

$$\rho_a(0) = \sum_{I,J=1}^{N} \alpha_{Ia}^2\alpha_{Ja}^2 = \sum_{I=1}^{N}\left(\sum_{J=1}^{N}\alpha_{Ja}^2\right)\alpha_{Ia}^2 = 1. \tag{5.6}$$

That is, $|\Psi(0)\rangle = |a\rangle$. Therefore, $\rho_a(t) \leq \rho_a(0)$ and $I_a(t) \leq I_a(0)$. But this can only be true in general if all the a-type phases are $+1$. Thus, the qualitative difference in phase behavior between a-type and non-a-type bands has clear meaning in terms of IVR. The presence of -1 phases in the decays of γ-type ($\gamma \neq a$) bands reflects the fact that vibrational energy will redistribute into the $|\gamma\rangle$ states as time increases. On the other hand, the fact that the amount of vibrational energy in $|a\rangle$ is at a maximum at $t = 0$ (by virtue of the exclusive absorption strength of $|a\rangle$) is reflected in the entirely positive phases of a-type decays.

A final utility of the correspondence between $I_\gamma(t)$ and $\rho_\gamma(t)$ is that it provides a means by which one can experimentally search for quasiperiodic and chaotic vibrational behavior in molecules. Being that such behaviors have been shown to be manifested in characteristically different ways in $\rho_\gamma(t)$,[18] then measurement of $I_\gamma(t)$ would be expected to provide information on the nature (i.e., quasiperiodic or chaotic) of the vibrational dynamics of a given molecule at a given energy. For more discussion on this see paper II, Sec. VI A.

B. Dependence of decay behavior on total vibrational energy

A number of published papers[1,14,19] have dealt with the effects of excess vibrational energy on large molecule IVR, as manifested in dispersed fluorescence spectra. From these studies, trends toward increasing spectral congestion and decreasing intensity in the unrelaxed region of the fluorescence spectra were observed as the vibrational energy was increased. These have been interpreted as being manifestations of faster and more extensive IVR at higher energies. Physically, this is reasonable since the average spacing of vibrational states decreases, and, thus, the opportunity for coupling increases with energy. However, the information available from purely spectral results is limited and can be misleading.[5] On the other hand, we have seen that fluorescence decay measurements can directly reveal a large amount of information about IVR. Thus, it is of interest to consider how time-resolved results might be expected to be dependent on excess vibrational energy and how they might correlate with the trends in dispersed fluorescence spectra.

As mentioned above, the principal expected modification of vibrational coupling with increasing vibrational energy is an average increase in the number of levels coupled to one another. The consideration of the changes in decay behavior with excess energy is, therefore, tantamount to the consideration of the changing nature of decays as N increases. Guided by experimental results,[6] we have found it useful to classify decays according to three ranges of N: (1) $N = 1$, (2) $N = 2$ to ~ 10, and (3) $N \geq 10$. These ranges of N may be identified with *low, intermediate,* and *high* vibrational energy regimes, respectively, in real molecules.

1. No IVR

The $N = 1$ case obviously corresponds to no IVR. The spectral manifestations of this are uncluttered spectra consisting of sharp vibronic bands assignable in terms of optically active vibrational intervals.[14(b)] The decays of all the bands in such a spectrum are *identical* and in most situations (i.e., barring any unusual nonradiative channels such as small energy gap intersystem crossing) will be single exponential and unmodulated.

2. Restricted IVR

The $N = 2$ to ~ 10 case corresponds to *restricted* IVR. A dispersed fluorescence spectrum belonging to this case consists of an uncongested, vibrationally unrelaxed region (see Sec. II D) composed of weak intensity a-type bands, and a congested, vibrationally relaxed region consisting primarily of non-a-type bands. The decays of the

various bands in the spectra adhere to the characteristics presented in Sec. II. They differ from the $N = 1$ case in that the decay behavior depends on detection wavelength, and that modulations are always present. The feature that distinguishes the decays of this case from those arising from systems of greater N is the presence of a number of essentially full recurrences on the timescale of the fluorescence lifetime. That is, each intensity $I_\gamma(t)$ [and each $\rho_\gamma(t)$] has a number of maxima, all of which approach the global maximum of that intensity. IVR is restricted in the sense that energy does not irreversibly flow from one vibration into others, but instead oscillates between a small number of levels.

3. Dissipative IVR

Finally, the case where N is large corresponds to *dissipative* IVR. Spectrally, this case is characterized by very weak a-type fluorescence bands in the unrelaxed region, and very congested, predominantly non-a-type fluorescence in the relaxed spectral region. Due to the large number of interference terms modulating fluorescence decays belonging to this case, the overall contribution of these terms is at a maximum at $t = 0$, after which a dephasing occurs which renders the contribution small for all subsequent times. For a-type decays, in which all the interference terms have $+1$ phases, this dephasing gives rise to a rapid initial decay component[5,20] followed by a long component of comparatively small intensity. For non-a-type decays, in which the initial intensity of zero arises from the -1 value for the sum of the modulation depths, the dephasing results in a rise time followed by a long decay. In both cases the possibility exists that some small modulations may occur on the long decay components; i.e., some partial recurrences may occur on the timescale of the fluorescence lifetime. However, the dephasing is sufficiently complete to exclude anything close to a full recurrence *on this time scale.* This type of decay behavior represents the irreversible flow of energy out of the initially prepared $|a\rangle$ excited state into the other coupled zero-order states.

Lahmani *et al.*[20] have shown (in the context of singlet-triplet coupling) that the decays corresponding to large N may be reproduced by assuming a kinetic rate equation model for the values $\rho_\gamma(t)$. For an a-type decay this model predicts a double exponential decay of the form

$$I_a(t) \sim \rho_a(t) = \frac{1}{N}[(N-1)e^{-(\Gamma+\Delta)t} + e^{-\Gamma t}], \tag{5.7}$$

where Γ is the same as in Sec. II, and Δ is a measure of the width of the distribution of beat frequencies and corresponds to the dephasing contribution to the decay. For non-a-type decays taken together the model gives

$$\sum_{\gamma \neq a} I_\gamma(t) \sim \sum_{\gamma \neq a} \rho_\gamma(t) = \frac{N-1}{N}[e^{-\Gamma t} - e^{-(\Gamma+\Delta)t}]. \tag{5.8}$$

These equations, by virtue of their very simplicity, serve several useful purposes. Firstly, they provide at a glance the general temporal behavior of IVR in the dissipative regime. Secondly, they serve as convenient functions with which one can fit experimental decays and thereby obtain IVR parameters. Thirdly, they relate in a simple way the parameter Δ to the rate of dissipative IVR. Δ, in turn, can be related[21] to molecular parameters such as the vibrational density of states and vibrational coupling matrix elements. Finally, their derivation by means of a kinetic model makes apparent the close analogy between IVR and kinetic behavior. In particular, one can meaningfully speak of $1/\Delta$ as an equilibration time during which a molecule, initially jarred out of equilibrium by the laser, evolves to a "steady state" in which no further evolution in the distribution of vibrational energy occurs.

One must, however, beware of taking Eqs. (5.7) and (5.8) too literally. Firstly, as pointed out in Ref. 20, the equations exclude the possibility of quantum beats. Secondly, Eq. (5.7) predicts that the ratio of the preexponential factors of fast to slow fluorescence for an a-type decay will be equal to $N - 1$, the number of states coupled to $|a\rangle$. However, by Eq. (2.13) one can see that the value $N - 1$ is actually an upper limit to this ratio, and it holds only if $|\alpha_{Ia}| = 1/N$, for all I.

VI. SUMMARY AND CONCLUSIONS

In this paper we have considered the dynamics of molecular vibrational energy flow between an arbitrary number of coupled vibrational levels. In particular, the concern has been centered on the dynamical manifestations of vibrational coupling in the temporal characteristics of spectrally resolved fluorescence. These manifestations take the form of coherence (phase-shifted quantum beats) in fluorescence decays, the number of beat frequencies in which is related to the number of coupled levels, and the beat phases and modulation depths in which are dependent on the fluorescence band detected. It has been shown that these phases and modulation depths are functions of the coefficients that connect the basis set of the zero-order, coupled vibrational wave functions to the molecular eigenstate basis set. As such, they are not arbitrary, but adhere to certain rules and restrictions ultimately based in the orthonormality of the mixing coefficients. Conversely, it has been shown that with knowledge of beat phases and modulation depths, it is possible to determine these coefficients, which when so determined, can then be used along with the beat frequencies to construct the Hamiltonian matrix describing the coupling between the zero-order vibrational states. Thus, the measurement of time- and frequency-resolved fluorescence can (1) indicate the presence of vibrational coupling in a molecule, (2) indicate the number of coupled levels, and (3) provide information leading to the determination of the details of the coupling.

It has also been shown in this paper that, more than just providing parameters pertinent to vibrational coupling, the temporal behavior of dispersed fluorescence has an immediate and simple interpretation in terms of IVR. The intensity vs time of a given band in a fluorescence spectrum is a direct picture of the evolution of vibrational energy in the excited state. Quantum beat frequencies are

related to the IVR time scale. Beat phases and modulation depths have straightforward interpretations in terms of the vibrational energy content of the excited state. And, most important, the nature of IVR at a particular vibrational energy is apparent from the decays of fluorescence bands. Thus, one can readily assess the transition from absent to restricted to dissipative IVR in a given molecule.

The results presented in this paper have been derived to facilitate the interpretation of real experimental data. In the following papers these theoretical results will be applied to new experimental observations made on the molecules anthracene[6] and *trans*-stilbene.[8]

ACKNOWLEDGMENT

This work was supported by the National Science Foundation through Grant No. DMR-8105034.

APPENDIX: SPECIFIC RESULTS FOR $N \leq 5$

As an illustration of the general concepts derived in Sec. II, and as a source of information on the coupling cases most amenable to study by quantum beat spectroscopy, we present in this Appendix specific results for $N \leq 5$.

1. $N = 2$

This case has been treated previously in part.[3,4] We include the results here for the sake of completeness. According to the theory presented above, one expects two types of bands (a and b type), and one beat frequency (ω_{12}) modulating both types of bands. The phase of the modulation of the a-type band will be $+1$ [i.e., $s_a(\omega_{12}) = +1$], while that of the b-type band will be -1 [i.e., $s_b(\omega_{12}) = -1$]. Furthermore, while by Eq. (2.17) $M_b(\omega_{12}) = -1$ and is coupling independent, $M_a(\omega_{12})$ is dependent on the coupling between the zero-order states. In fact, it is a simple matter, given the following definition for the Hamiltonian matrix in the zero-order basis:

$$H_0 \equiv \begin{pmatrix} E_a & V_{ab} \\ V_{ab} & E_b \end{pmatrix}, \tag{A1}$$

TABLE I. A summary of results for $N = 3$.

No. of band types	No. of beat frequencies	No. of beat triplets
3	3	1

Four possible quantum beat phase distributions:

	Independent phases		Dependent phase
Distribution	$S_\gamma(\omega_{12})$	$S_\gamma(\omega_{13})$	$S_\gamma(\omega_{23})$
δ_γ^1	+1	+1	+1
δ_γ^2	+1	−1	−1
δ_γ^3	−1	+1	−1
δ_γ^4	−1	−1	+1

TABLE II. A summary of results for $N = 4$.

No. of band types	No. of beat frequencies	No. of beat triplets
4	6	4

Eight possible quantum beat phase distributions:

	Independent phases			Dependent phases		
Distribution	$S_\gamma(\omega_{12})$	$S_\gamma(\omega_{13})$	$S_\gamma(\omega_{14})$	$S_\gamma(\omega_{23})$	$S_\gamma(\omega_{24})$	$S_\gamma(\omega_{34})$
δ_γ^1	+1	+1	+1	+1	+1	+1
δ_γ^2	+1	−1	−1	−1	−1	+1
δ_γ^3	−1	+1	−1	−1	+1	−1
δ_γ^4	−1	−1	+1	+1	−1	−1
δ_γ^5	+1	−1	+1	−1	+1	−1
δ_γ^6	+1	+1	−1	+1	−1	−1
δ_γ^7	−1	+1	+1	−1	−1	+1
δ_γ^8	−1	−1	−1	+1	+1	+1

to show that the a-type modulation depth is

$$M_a(\omega_{12}) = \frac{1}{2R^2 + 1}, \tag{A2}$$

where $R \equiv |(E_a - E_b)/2V_{ab}|$. Because

$$\hbar\omega_{12} = 2|V_{ab}|(R^2 + 1)^{0.5}, \tag{A3}$$

then the measurement of ω_{12} and $M_a(\omega_{12})$ allows one to obtain the zero-order energy difference $|E_a - E_b|$ and the magnitude of the coupling matrix element $|V_{ab}|$.

2. $N = 3$

For $N = 3$ one expects three types of bands (a, b, and c type) in the dispersed fluorescence spectrum. Each will be modulated by the three beat frequencies ω_{12}, ω_{23}, and ω_{13} ($=\omega_{12} + \omega_{23}$). One also expects four possible quantum beat phase distributions for these bands. Unlike the case of $N = 2$, all $M_\gamma(\omega_{IJ})$ values are coupling dependent (i.e., $\alpha_{I\gamma}$ dependent) for $N = 3$ (and for $N > 3$). It is only the sum of modulation depths for any given non-a-type band which is coupling independent [cf. Eq. (2.17)]. A summary of results for $N = 3$ appears in Table I. (Note that in Tables I–III we have labeled specific phase distributions. Note also that in Tables I and II we have included the dependent quantum beat phases as well as the independent part δ_γ.)

3. $N = 4$

A summary of information for $N = 4$, including possible beat phase distributions, is contained in Table II. For this case and for $N > 4$ there are additional restrictions on the phase distributions, which do not appear for $N \leq 3$ and which were not addressed in the general treatment of Sec. II C. These restrictions derive from the condition that $\sigma^I \neq \sigma^J$, for $I \neq J$, and they limit the combinations of δ_γ which can appear in a given spectrum. As an example, consider the phase distributions δ_γ^1, δ_γ^2, δ_γ^7, and δ_γ^8 from Table II, and assume that they correspond to the a-, b-, c-, and d-type bands, respectively,

TABLE III. A summary of results for $N = 5$.

No. of band types	No. of beat frequencies	No. of beat triplets
5	10	10

16 possible quantum beat phase distributions:

	Independent		Phases	
Distribution	$S_\gamma(\omega_{12})$	$S_\gamma(\omega_{13})$	$S_\gamma(\omega_{14})$	$S_\gamma(\omega_{15})$
1	+1	+1	+1	+1
2	+1	+1	+1	−1
3	+1	+1	−1	+1
4	+1	−1	+1	+1
5	−1	+1	+1	+1
6	+1	+1	−1	−1
7	+1	−1	+1	−1
8	−1	+1	+1	−1
9	+1	−1	−1	+1
10	−1	+1	−1	+1
11	−1	−1	+1	+1
12	+1	−1	−1	−1
13	−1	+1	−1	−1
14	−1	−1	+1	−1
15	−1	−1	−1	+1
16	−1	−1	−1	−1

in the spectrum of a 4-level system. Using these distributions and Eq. (2.27), one obtains

$$\text{sign}(C) = \begin{pmatrix} 1 & 1 & 1 & 1 \\ 1 & 1 & -1 & -1 \\ 1 & -1 & 1 & 1 \\ -1 & 1 & 1 & 1 \end{pmatrix}, \tag{A4}$$

where each row of the matrix is determined up to an overall sign. Now, although $\sigma_\gamma \neq \sigma_{\gamma'}$ in Eq. (A4), $\sigma^3 = \sigma^4$, contrary to the restrictions on the σ^{I}'s (2.24). Thus, the combination of δ^1_γ, δ^2_γ, δ^7_γ, and δ^8_γ, cannot correspond to bands in the same spectrum. Five other such forbidden combinations of phase distributions exist for $N = 4$. We shall not deal any further with the specifics of these forbidden combinations except to note, again, that they are present for all N greater than three.

4. $N = 5$

A summary of results for $N = 5$ is presented in Table III.

[1] For a review see: C. S. Parmenter, Faraday Discuss. Chem. Soc. **75,** 7 (1983).

[2] P. M. Felker and A. H. Zewail, in *Applications of Picosecond Spectroscopy to Chemistry,* edited by K. B. Eisenthal (Reidel, Dortrecht, 1984), p. 273.

[3] P. M. Felker and A. H. Zewail, Chem. Phys. Lett. **102,** 113 (1984).

[4] P. M. Felker and A. H. Zewail, Phys. Rev. Lett. **53,** 501 (1984).

[5] P. M. Felker and A. H. Zewail, Chem. Phys. Lett. **108,** 303 (1984).

[6] P. M. Felker and A. H. Zewail, J. Chem. Phys. **82,** 2975 (1985).

[7] P. M. Felker and A. H. Zewail, J. Chem. Phys. **82,** 2994 (1985).

[8] P. M. Felker, W. R. Lambert, and A. H. Zewail, J. Chem. Phys. **82,** 3003 (1985).

[9] We assume here that all of the matrix elements of H_0, the Hamiltonian matrix in the zero-order basis, can be expressed as real numbers, in which case all the elements of C can be taken as real.

[10] See, for example: S. Haroche, in *High Resolution Laser Spectroscopy,* edited by K. Shimoda (Springer, New York, 1976), p. 254.

[11] Since all the excited eigenstates are S_1 levels of about the same energy, one does not expect Γ to vary much from level to level. Taking Γ to be equal for all levels is therefore a reasonable approximation. It is pertinent to note that even if Γ were not the same for all eigenstates, this would not affect the beat phases or modulation depths in a given decay.

[12] Examples are the spectra of anthracene appearing in W. R. Lambert, P. M. Felker, J. A. Syage, and A. H. Zewail, J. Chem. Phys. **81,** 2195 (1984).

[13] This is a different situation from that which obtains in, for example, Zeeman quantum beats, where beat phases and modulations depend on the polarizations of the excitation source and detection analyzer, as well as on the magnetic field direction. This is the case because the Zeeman quantum beats arise as an interference effect between two magnetic sublevels, which sublevels have different polarization characteristics. On the other hand, the beats described herein arise from interferences between states which have the same Zeeman quantum number (M_J). A discussion of polarization effects on molecular quantum beats may be found in M. Bixon, J. Jortner, and Y. Dothan, Mol. Phys. **17,** 109 (1969). For experimental results on Zeeman quantum beats see, for example, Ref. 10; and R. Wallenstein, J. A. Paisner, and A. L. Schawlow, Phys. Rev. Lett. **32,** 1333 (1974).

[14] See, for example: (a) G. Stewart, M. Ensminger, T. Kulp, R. Ruoff, and J. D. McDonald, J. Chem. Phys. **79,** 3190 (1983); (b) S. M. Beck, J. B. Hopkins, D. E. Powers, and R. E. Smalley, J. Chem. Phys. **74,** 43 (1981).

[15] The analysis of *time-integrated* observables to obtain molecular Hamiltonian matrices in zero-order basis sets has been performed by a number of other researchers: (a) J. E. Wessel, Ph.D. thesis, University of Chicago, 1970; (b) J. Wessel and D. S. McClure, Mol. Cryst. Liq. Cryst. **58,** 121 (1980); (c) C. A. Langhoff and G. W. Robinson, Chem. Phys. **6,** 34 (1974); (d) B. M. van der Meer, H. Th. Jonkman, and J. Kommandeur, in *Photochemistry and Photobiology, Vol. 1,* edited by A. H. Zewail (Harwood Academic, Chur, Switzerland, 1983), p. 77. Our thrust in Sec. III is to show how such an analysis may be made using time-resolved, phase-shifted quantum beat data. We would note two significant differences between the two types of analyses. Analyses such as those made in (a)–(d) must make an assumption that observed perturbed spectra arise from coherent coupling interactions, and not from the inhomogeneous superposition of dynamically unrelated spectra; e.g., the different spectra arising from different rotational levels. No such assumption need be made in the case we treat in Sec. III, since the existence of phase-shifted beats implies the presence of a coherent coupling interaction between levels. Secondly, we note that the analyses in (a)–(d) must assume a prediagonalized set of zero-order "bath" states, because bath states are not observed by the experimental techniques upon which they rely, and therefore there is not enough information to give the details of the coupling between bath states. Prediagonalization is not necessary using phase-shifted quantum beats, since information pertaining to the couplings of all zero-order states is contained in the beating decays of the different fluorescence bands, including those arising from bath states.

[16] G. Herzberg, *Infrared and Raman Spectra of Polyatomic Molecules* (Van Nostrand, Princeton, 1945), p. 216.

[17] W. Rhodes, in *Radiationless Transitions,* edited by S. H. Lin (Academic, New York, 1980), p. 219.

[18] See, for example: (a) G. Hose and H. S. Taylor, Chem. Phys. **84,** 375 (1984); (b) M. D. Feit and J. A. Fleck, Jr., J. Chem. Phys. **80,** 2578 (1984); and references therein.

[19] For example: (a) P. S. H. Fitch, L. Wharton, and D. Levy, J. Chem. Phys. **70,** 2018 (1979); (b) A. Amirav, U. Even, and J. Jortner, *ibid.* **74,** 3475 (1981); (c) C. Bouzou, C. Jouvet, J. B. Leblond, Ph. Millie, A. Tramer, and M. Sulkes, Chem. Phys. Lett. **97,** 61 (1983); (d) M. Fujii, T. Ebata, N. Mikami, M. Ito, S. H. Kable, W. D. Lawrance, T. B. Parsons, and A. E. W. Knight, J. Phys. Chem. **81,** 2209 (1984).

[20] F. Lahmani, A. Tramer, and C. Tric, J. Chem. Phys. **60,** 4431 (1974).

[21] C. Tric, Chem. Phys. **14,** 189 (1976).